

ORIGINAL ARTICLE

Brain-Derived Neurotrophic Factor Improves Impaired Fatty Acid Oxidation Via the Activation of Adenosine Monophosphate-Activated Protein Kinase- α – Proliferator-Activated Receptor- γ Coactivator-1 α Signaling in Skeletal Muscle of Mice With Heart Failure

Junichi Matsumoto, MD, PhD*¹; Shingo Takada¹, PhD*¹; Takaaki Furihata¹, MD, PhD¹; Hideo Nambu, MD, PhD¹; Naoya Kakutani, PhD¹; Satoshi Maekawa¹, MD, PhD¹; Wataru Mizushima, MD, PhD¹; Ippei Nakano¹, MD, PhD¹; Arata Fukushima, MD, PhD¹; Takashi Yokota¹, MD, PhD¹; Shinya Tanaka¹, MD, PhD¹; Haruka Handa¹, MD, PhD¹; Hisataka Sabe, PhD¹; Shintaro Kinugawa¹, MD, PhD¹



BACKGROUND: We recently reported that treatment with rhBDNF (recombinant human brain-derived neurotrophic factor) improved the reduced exercise capacity of mice with heart failure (HF) after myocardial infarction (MI). Since BDNF is reported to enhance fatty acid oxidation, we herein conducted an in vivo investigation to determine whether the improvement in exercise capacity is due to the enhancement of the fatty acid oxidation of skeletal muscle via the AMPK α -PGC1 α (adenosine monophosphate-activated protein kinase- α -proliferator-activated receptor- γ coactivator-1 α) axis.

METHODS: MI and sham operations were conducted in C57BL/6J mice. Two weeks postsurgery, we randomly divided the MI mice into groups treated with rhBDNF or vehicle for 2 weeks. AMPK α -PGC1 α signaling and mitochondrial content in the skeletal muscle of the mice were evaluated by Western blotting and transmission electron microscopy. Fatty acid β -oxidation was examined by high-resolution respirometry using permeabilized muscle fiber. BDNF-knockout mice were treated with 5-aminoimidazole-4-carboxamide-1- β -D-ribofuranoside, an activator of AMPK.

RESULTS: The rhBDNF treatment significantly increased the expressions of phosphorylated AMPK α and PGC1 α protein and the intermyofibrillar mitochondrial density in the MI mice. The lowered skeletal muscle mitochondrial fatty acid oxidation was significantly improved in the rhBDNF-treated MI mice. The reduced exercise capacity and mitochondrial dysfunction of the BDNF-knockout mice were improved by 5-aminoimidazole-4-carboxamide-1- β -D-ribofuranoside.

CONCLUSIONS: Beneficial effects of BDNF on the exercise capacity of mice with HF are mediated through an enhancement of fatty acid oxidation via the activation of AMPK α -PGC1 α in skeletal muscle. BDNF may become a therapeutic option to improve exercise capacity as an alternative or adjunct to exercise training.

Key Words: brain-derived neurotrophic factor ■ heart failure ■ mitochondria ■ myocardial infarction ■ skeletal muscle

Correspondence to: Shintaro Kinugawa, MD, PhD, Department of Cardiovascular Medicine, Faculty of Medicine and Graduate School of Medicine, Hokkaido University, Kita-15, Nishi-7, Kita-ku, Sapporo 060-8638, Japan. Email tuckahoe@med.hokudai.ac.jp

*Drs Matsumoto and Takada contributed equally to this work.

The Data Supplement is available at <https://www.ahajournals.org/doi/suppl/10.1161/CIRCHEARTFAILURE.119.005890>.

For Sources of Funding and Disclosures, see page xxx.

© 2020 American Heart Association, Inc.

Circulation: Heart Failure is available at www.ahajournals.org/journal/circheartfailure

WHAT IS NEW?

- Brain-derived neurotrophic factor (BDNF) is abundantly expressed in slow-twitch fibers and colocalized with mitochondria.
- Beneficial effects of BDNF on exercise capacity of mice with heart failure after myocardial infarction was mediated through an enhancement of fatty acid oxidation via the activation of AMPK α -PGC1 α signaling in the skeletal muscle.
- Treatment with BDNF had the same effects as aerobic exercise training on exercise capacity and molecular levels of the skeletal muscle.

WHAT ARE THE CLINICAL IMPLICATIONS?

- With the aging of societies, the number of elderly patients with heart failure is increasing rapidly. New treatment strategies aimed at improving exercise capacity are needed, but there is currently no established drug therapy. Treatment with BDNF offers potential benefit in improving exercise capacity in patients with heart failure.
- Treatment with BDNF may be an alternative or an adjunct to aerobic exercise training for patients with heart failure who have severely impaired activities of daily living and cannot perform sufficient aerobic exercise training.

Nonstandard Abbreviations and Acronyms

AMPKα	adenosine monophosphate-activated protein kinase- α
AICAR	5-aminoimidazole-4-carboxamide-1-beta-d-ribofuranoside
BDNF	brain-derived neurotrophic factor
BW	body weight
CPT	carnitine palmitoyl-transferase
CS	citrate synthase
ET	exercise training
ETF	electron transfer flavoprotein
HF	heart failure
MI	myocardial infarction
PGC1α	proliferator-activated receptor-coactivator-1 α
rhBDNF	recombinant human brain-derived neurotrophic factor
SDH	succinic dehydrogenase
SED	sedentary conditions
WT	wild type

The reduced exercise capacity of individuals who have experienced heart failure (HF) is due mainly to skeletal muscle abnormalities.^{1,2} These abnormalities include impaired energy metabolism, mitochondrial dysfunction, a fiber-type switch from

oxidative fibers to glycolytic fibers, and skeletal muscle atrophy.^{1,2} Mitochondrial enzymes, including fatty acid β -oxidation enzymes, are reduced in the skeletal muscles of patients with HF.³ Our investigation using magnetic resonance spectroscopy revealed that an increased accumulation of intramyocellular lipid was closely associated with muscle energy production and exercise capacity.⁴ As an intervention for such metabolic alterations, exercise training (ET) is the only therapy that has been shown to improve subjects' reduced exercise capacity and impaired fatty acid metabolism in the skeletal muscle, and ET can prolong survival in patients with HF. Therefore, therapeutic strategies that can mimic the metabolic effects of ET would be highly beneficial in the HF setting.

BDNF (brain-derived neurotrophic factor) is a member of the neurotrophic family of growth factors.⁵⁻⁷ It is present in the nervous system, and it promotes the neuronal system's growth, development, maintenance of functions, and survival.⁵⁻⁷ We demonstrated that serum BDNF levels were decreased in patients with HF in association with lower peak oxygen uptake.⁸ We also confirmed that decreased serum BDNF levels predicted adverse clinical outcomes in patients with HF.⁹ Other authors have shown that exercise increases both circulating and skeletal muscle BDNF levels,¹⁰ which raises the possibility that BDNF secretion from the skeletal muscles influences the circulating BDNF levels.

We recently established that in a mouse HF model after myocardial infarction (MI), the BDNF protein expression in the skeletal muscle is decreased; we also observed that treatment with rhBDNF (recombinant human BDNF) improved the reduced aerobic exercise capacity and mitochondrial dysfunction in the skeletal muscles of the HF mice.¹¹ These results suggested that BDNF in the skeletal muscle is closely associated with the body's aerobic capacity, and that BDNF pharmacological therapy could be a good candidate for an alternative to for exercise therapy.

The presence of AMPK α and PGC1 α , which are master regulators of mitochondrial function, is greater in slow-twitch muscle fibers. Exercise enhances mitochondrial biogenesis and fatty acid oxidation in the skeletal muscle via the AMPK α -PGC1 α pathway.¹² BDNF enhances PGC1 α -mediated mitochondrial biogenesis in hippocampal neurons.¹³ In addition, BDNF enhances fatty acid oxidation *in vitro* (in intact L6 myotubes) and *in vivo* (in isolated intact rat skeletal muscle) via the activation of AMPK α signaling.¹⁰ Taken together, these findings indicated that BDNF may be closely linked to the AMPK α -PGC1 α axis.

The mechanism by which an administration of BDNF increases the exercise capacity of mice with HF had been unknown. We hypothesized that the beneficial effect of BDNF on the exercise capacity of HF mice was attributable to the enhancement of

skeletal muscle mitochondrial fatty acid oxidation via the activation of AMPK α -PGC1 α signaling. We thus conducted the present *in vivo* study to clarify this issue. Our results indicate that the beneficial effects of BDNF on the exercise capacity of HF mice are indeed mediated through an enhancement of fatty acid oxidation via the activation of AMPK α -PGC1 α in skeletal muscle.

METHODS

All experiments and methods of animal care were performed according to the Guide for the Care and Use of Laboratory Animals of the US National Institutes of Health and approved by our institutional animal research committee; they also conformed to the Animal Care Guidelines for the Care and Use of Laboratory Animals of the Hokkaido University Graduate School of Medicine. All data and materials supporting the findings of this study are available within the article and in the [Data Supplement](#) or from the corresponding author upon reasonable request.

Experimental Animals

Male C57BL/6J mice were kept in a pathogen-free environment and housed in an animal room under a 12/12 hr light-dark cycle at a temperature of 23°C to 25°C with chow and tap water *ad libitum*. Mice were anesthetized with a combination anesthesia: 0.3 mg/kg body weight (BW) of medetomidine (Dorbene; Kyoritsuseiyaku Co, Tokyo), 4.0 mg/kg BW of midazolam (Dormicum; Astellas Pharma, Tokyo), and 5.0 mg/kg BW of butorphanol (Vetorphale; Meiji Seika, Tokyo) via intraperitoneal administration.¹⁴ MI was created by ligating the left coronary artery of the 10- to 12-week-old mouse weighing 23 to 26 g, as described previously.¹⁵ The sham operation was performed without ligating the coronary artery.

Study Protocol

Two weeks after the surgery, we randomly divided the MI mice and sham mice into 2 groups: treatment with rhBDNF (5 mg/kg BW/d) and treatment with vehicle (PBS) by subcutaneous injection for an additional 2 weeks. Four weeks after the operation (at the end of the 2-week treatments), the 4 groups of mice (ie, the sham+vehicle, sham+rhBDNF, MI+vehicle, and MI+rhBDNF mice [$n=7$ each]) were subjected to a treadmill test, and other experiments were performed in the 3 groups other than the sham+rhBDNF. Next, under deep anesthesia with the above-described combination of anesthesia, the mouse was euthanized, and its hindlimb skeletal muscle was excised, weighed, and used for the measurement of mitochondrial respiration and other experiments.

Echocardiographic Measurement

Transthoracic echocardiography was performed using an Aplio 300 ultrasound machine (Toshiba Medical Systems, Otawara, Japan) equipped with a 12-MHz linear transducer as described previously.¹⁵ We conducted the echocardiography with the mouse in the conscious state to avoid a potential influence of anesthesia on cardiac function.¹⁶

Exercise Capacity and Spontaneous Physical Activity

We subjected the mice to a treadmill exercise test using a motorized treadmill (Oxymax 2; Columbus Instruments, Columbus, OH) as described previously.¹⁷ In brief, after a resting period of 10 minutes, the mouse was provided a 10-minute warm-up period at 6 m/min at 0° inclination. After warming up, the mouse ran on a graded treadmill at a 10° incline; the speed was incrementally increased by 2 m/min every 2 minutes until exhaustion. Exhaustion was defined as spending time (≥ 10 seconds) on the shocker plate without attempting to re-engage the treadmill. Spontaneous physical activity for 24 hours was measured using an animal movement analysis system (ACTIMO System; Shintech, Fukuoka, Japan) as described previously.^{15,18}

Mitochondrial Respiration With Fatty Acid Substrates

The methods used to prepare permeabilized fibers and the measurement of mitochondrial respiration were as described previously.¹⁵ In brief, the red portion of the gastrocnemius muscle was quickly excised and immediately placed in ice-cold biopsy preservation solution containing 2.77 mmol/L CaK₂ EGTA, 7.23 mmol/L EGTA, 20 mmol/L taurine, 0.56 mmol/L MgCl₂, 5.77 mmol/L ATP, 15 mmol/L phosphocreatine, 0.5 mmol/L DTT, and 50 mmol/L MOPS, pH 7.1. After permeabilization using 0.05 mg/mL saponin solution, we transferred the permeabilized fiber (1.5–3.0 mg) to a thermostat (37°C) chamber and started to measure the mitochondrial respiration.

The mitochondrial respiratory capacity was measured by high-resolution respirometry (Oxygraph-2k; Oroboros Instruments, Innsbruck, Austria) in MiRO5 medium (0.5 mmol/L EGTA, 110 mmol/L sucrose, 60 mmol/L potassium lactobionate, 20 mmol/L taurine, 3 mmol/L MgCl₂·6H₂O, 10 mmol/L KH₂PO₄, 20 mmol/L HEPES, and 1 g/L BSA, pH 7.1). We conducted a protocol with fatty acid substrates as follows: (1) malate 2 mmol/L, (2) octanoyl-L-carnitine 0.15 mmol/L, (3) ADP-Mg 5 mmol/L, and (4) cytochrome c 10 μ mol/L. We tested the integrity of the outer mitochondrial membrane by adding cytochrome c, and the data were eliminated when the increase in the oxygen consumption rate was $>10\%$ as a sign of a damaged outer mitochondrial membrane. Datlab software ver.6 (Oroboros Instruments) was used for the data acquisition and data analysis.

BDNF^{+/-} Mice

BDNF hetero-knockout (BDNF^{+/-}) and BDNF^{+/+} (wild type [WT]) mice were purchased from Jackson Laboratories (Bar Harbor, ME). Hindlimb skeletal muscle was excised as described above and used for Western blotting and mitochondrial DNA analyses. Next, 5-aminoimidazole-4-carboxamide-1-beta-d-ribofuranoside (AICAR; Toronto Research Chemicals, Ontario, Canada) at 500 mg/kg BW/d or vehicle (saline) was intraperitoneally injected into BDNF^{+/-} mice for 5 weeks, and the treadmill test was performed, and CS (citrate synthase) activity was measured using WT+vehicle mice ($n=8$), BDNF^{+/-}+vehicle mice ($n=7$), and BDNF^{+/-}+AICAR mice ($n=6$).

ET and the Administration of rhBDNF to Sedentary Mice

Male C57BL/6J mice maintained under sedentary conditions (SED) were subcutaneously injected with rhBDNF (10 mg/kg BW/d) or vehicle (PBS) for 5 weeks. The training groups then completed 5 weeks of swimming ET for 90 min/d, 5 d/wk.¹⁹ At the end of 5 weeks, the treadmill test was performed in SED+vehicle mice (n=11), SED+rhBDNF mice (n=5), and ET+vehicle mice (n=10).

C2C12 Cell Culture

C2C12 cells (ATCC CRL-1772) were cultured as described previously.²⁰ Fully differentiated C2C12 myotubes were also treated with rhBDNF (100 ng/mL), compound C (a potent and selective inhibitor of AMPK, 40 μ mol/L in DMSO; Calbiochem, Darmstadt, Germany), or a combination of rhBDNF and compound C for 30 minutes. Other fully differentiated C2C12 myotubes were treated with rhBDNF (100 ng/mL), anti-TrkB receptor antibody (1 μ g/mL in DMSO; Sigma-Aldrich, St. Louis, MO), or a combination of rhBDNF and anti-TrkB receptor antibody for 30 minutes.

The details of experimental methods for the Western blotting, immunohistochemical staining, measurement of CS activity, transmission electron microscopy, mitochondrial DNA analysis, quantitative real-time polymerase chain reaction, and immunofluorescence microscopy are provided in the [Data Supplement](#).

Statistical Analyses

Data are expressed as the mean \pm SD. The statistical analyses were performed using Student unpaired *t* test for comparisons of pairs of groups and a 1-way ANOVA followed by Tukey test for comparisons of 3 groups. The statistical analyses were performed using a 2-way ANOVA for comparisons of 4 groups with 2 factors and when there was an interaction effect between 2 factors, followed by Tukey test. Analyses were performed with GraphPad Prism 7 software (GraphPad, La Jolla, CA). *P* values <0.05 were considered significant.

RESULTS

BDNF Was Abundant in Slow Oxidative Skeletal Muscle Fibers of the Mice

We first assessed the tissue localization of BDNF in the skeletal muscles of the mice. The BDNF protein expression was significantly higher in soleus muscle (which is mainly type I, oxidative, slow-twitch fibers) than in gastrocnemius muscle (which is mainly type II, glycolytic, fast-twitch fibers) as evaluated by both Western blotting (Figure 1A) and immunohistochemistry staining (Figure 1B). We further assessed the BDNF expressions in the gastrocnemius muscle, which contains both a red part (type I fibers) and a white part (type II fibers). BDNF was highly expressed in the type I fibers, which were darkly stained with SDH (succinic dehydrogenase) compared with the type II fibers (Figure 1C). The soleus muscle had a higher proportion of type I fibers, and BDNF

expression was distributed throughout the soleus muscle (Figure I in the [Data Supplement](#)). Super-resolution microscopy showed that in the C2C12 myotubes, BDNF was co-localized with mitochondria (Figure 1D).

rhBDNF Treatment Improved the Exercise Capacity of MI Mice

In preliminary experiments, we used C57BL/6J mice to determine the dose of rhBDNF. The work tended to be increased in the C57BL/6J mice treated with 5 or 10 mg/kg BW/d for 2 weeks and was significantly increased in the C57BL/6J mice treated with 20 mg/kg BW/d for 2 weeks, and no obvious dose-dependent effects were observed (Figure II in the [Data Supplement](#)). When rhBDNF was administered at \geq 20 mg/kg BW/d, significant BW loss was observed in the mice (data not shown), and its efficacy on exercise capacity could not be verified.

The characteristics of the groups are summarized in Table I in the [Data Supplement](#). The BW was significantly decreased in the MI+rhBDNF mice compared with the other 2 groups. There was no significant difference in food intake among the groups. There were no significant differences in the heart, lung, and skeletal muscle weights between MI+vehicle and MI+rhBDNF mice. There were also no statistical differences in echocardiographic findings between MI+vehicle and MI+rhBDNF mice.

There was no significant differences in the exercise capacity between sham+vehicle and MI+rhBDNF mice (Figure 2A). We, therefore, performed other experiments in only the sham+vehicle, MI+vehicle, and MI+rhBDNF mice. The total running time and running distance were significantly lower in the MI+vehicle mice compared with the sham+vehicle mice, and these parameters were significantly improved in the MI+rhBDNF mice (Figure 2A). There was no significant difference in the spontaneous physical activity among groups (Figure 2B).

rhBDNF Treatment Improved the Mitochondrial Biogenesis and Function in Skeletal Muscle From MI Mice

We confirmed that the endogenous levels of BDNF in the skeletal muscle were decreased in the MI mice compared with the sham mice (Figure III in the [Data Supplement](#)). We evaluated the upstream signaling and mitochondrial content in skeletal muscles of the mice. The administration of rhBDNF significantly increased the protein expressions of phosphorylated AMPK α and PGC1 α (Figure 3A). Representative transmission electron microscopy images of the skeletal muscle from each group are shown in Figure 3B. The intermyofibrillar mitochondrial density was significantly decreased in the MI+vehicle mice, and this decrease was significantly ameliorated in the MI+rhBDNF mice (Figure 3B).

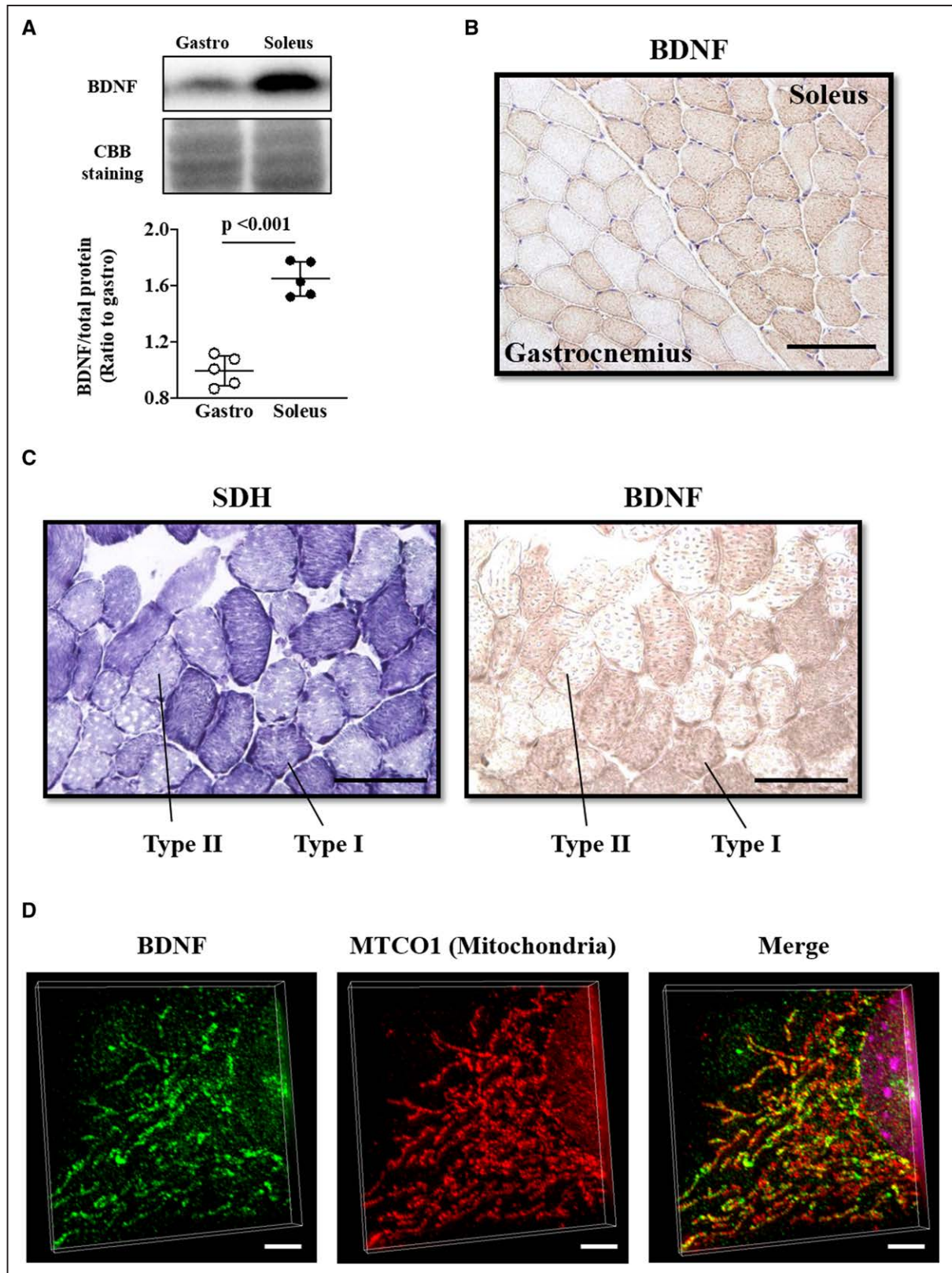


Figure 1. BDNF (brain-derived neurotrophic factor) was abundant in mouse type I fibers and co-localized with mitochondria. **A**, Representative Western blots and summary data of BDNF protein expressions in gastrocnemius muscle and soleus muscle. n=5 per group. **B**, A representative immunohistochemical staining image for BDNF in a slice of skeletal muscle including gastrocnemius and soleus muscle. Scale bar, 100 μ m. **C**, Representative immunohistochemical staining images for SDH (succinic dehydrogenase) and BDNF in the medial gastrocnemius muscle. The left and right panels show the results of staining with serial sections. Scale bar, 100 μ m. **D**, Representative super-resolution fluorescence microscopic images of C2C12 cells using antibodies to BDNF (green) and MTCO1 (mitochondrially encoded cytochrome c oxidase 1, red, a mitochondrial marker), and a merged image (yellow). Scale bar, 5 μ m. Data are mean \pm SD. CBB indicates coomassie brilliant blue.

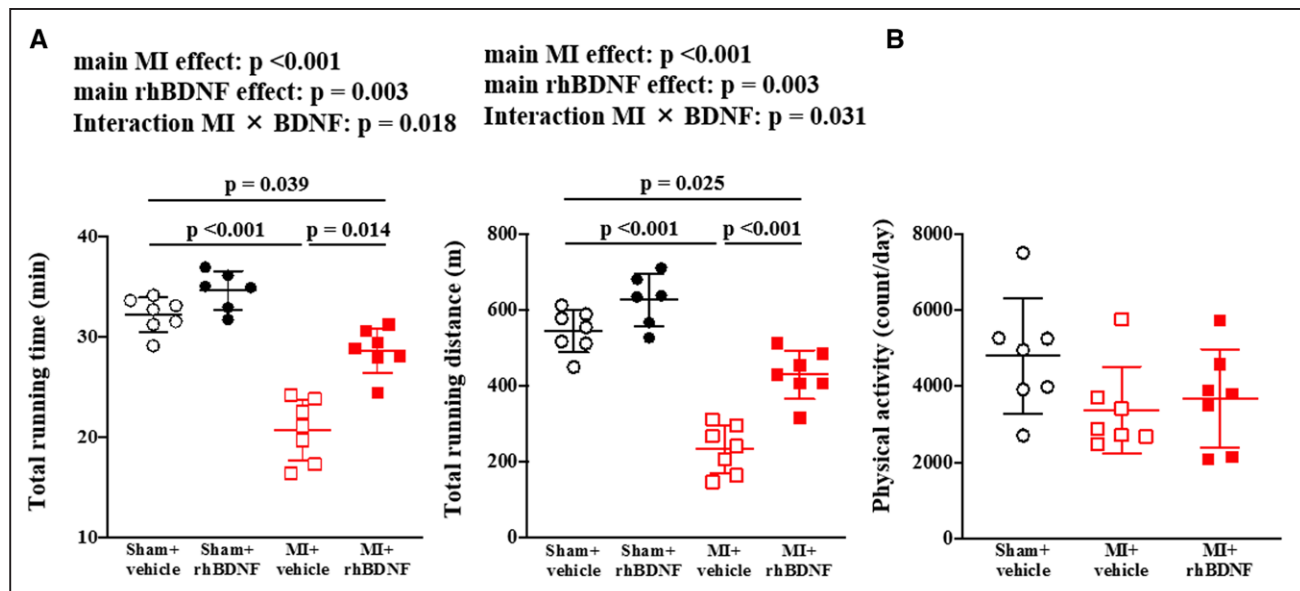


Figure 2. Treatment with rhBDNF (recombinant human brain-derived neurotrophic factor) improved the exercise capacity of myocardial infarction (MI) mice.

A, Total running time and running distance to exhaustion. **B**, Spontaneous physical activity. $n=7$ per group. Data are mean \pm SD.

An AMPK Activator Improved the Exercise Capacity of the BDNF^{+/-} Mice

To test our observations regarding AMPK α -PGC1 α signaling in BDNF treatment, we performed experiments using BDNF^{+/-} mice. As expected, the expression of BDNF was decreased in BDNF^{+/-} mice compared with the WT mice (Figure 4A). The levels of both phosphorylated AMPK α and PGC1 α were also decreased in the BDNF^{+/-} mice compared with the WT mice (Figure 4A). Consequently, mitochondrial DNA was decreased in the BDNF^{+/-} mice compared with the WT mice (Figure 4A), which suggests that mitochondrial content was decreased in the BDNF^{+/-} mice.

We investigated the effects of AICAR, a specific activator of AMPK, in BDNF^{+/-} mice. There were no significant differences in BW, organ weights, or echocardiographic parameters among the WT, BDNF^{+/-}, and BDNF^{+/-}+AICAR mice (data not shown). The total running time and total running distance were significantly lower in the BDNF^{+/-} mice compared with the WT mice (Figure 4B). The CS activity in the skeletal muscle was significantly lower in the BDNF^{+/-} mice compared with the WT mice (Figure 4C). The administration of AICAR improved the exercise capacity and CS activity in the skeletal muscle of the BDNF^{+/-} mice (Figure 4B and 4C).

BDNF Regulated Fatty Acid Metabolism

Mitochondrial fatty acid oxidation in the skeletal muscle was significantly lower in the MI+vehicle mice compared with the sham+vehicle mice, and it was significantly improved in the MI+rhBDNF mice compared with the

MI+vehicle mice (Figure 5A). The visceral fat weight was significantly lower in the MI+rhBDNF mice than the other 2 groups (Figure 5B). The protein expressions of CD36, CPT (carnitine palmitoyl-transferase) 1B, and CPT2 were significantly lower in the skeletal muscle from the MI+vehicle mice compared with the sham+vehicle mice, and these proteins were significantly up-regulated in the MI+rhBDNF mice compared with the MI+vehicle mice (Figure 5C). The expressions of the 2 proteins ETF α and ETF β (ETF [electron transfer flavoprotein] subunit α and subunit β) were significantly lower in the skeletal muscle from the MI+vehicle mice compared with that of the sham+vehicle mice, and these proteins were significantly up-regulated by rhBDNF (Figure 5C). The number of intramyocellular lipid droplets was significantly increased in the MI+vehicle mice compared with the sham+vehicle, and rhBDNF treatment significantly decreased this number (Figure 5D).

rhBDNF Treatment Increased the Exercise Capacity of Sedentary Mice

We determined the effects of BDNF on exercise capacity and mitochondrial function in skeletal muscle in normal mice (sedentary mice) and compared these effects with those of ET. The rhBDNF treatment of sedentary mice for 5 weeks significantly increased both their exercise capacity and the CS activity in their skeletal muscle, which was comparable with the effects of ET (Figure 6A and 6B). Consistent with the increased exercise capacity, rhBDNF increased the expressions of genes in the skeletal muscle that are related to the tricarboxylic acid cycle, electron transport chain, mitochondrial biogenesis,

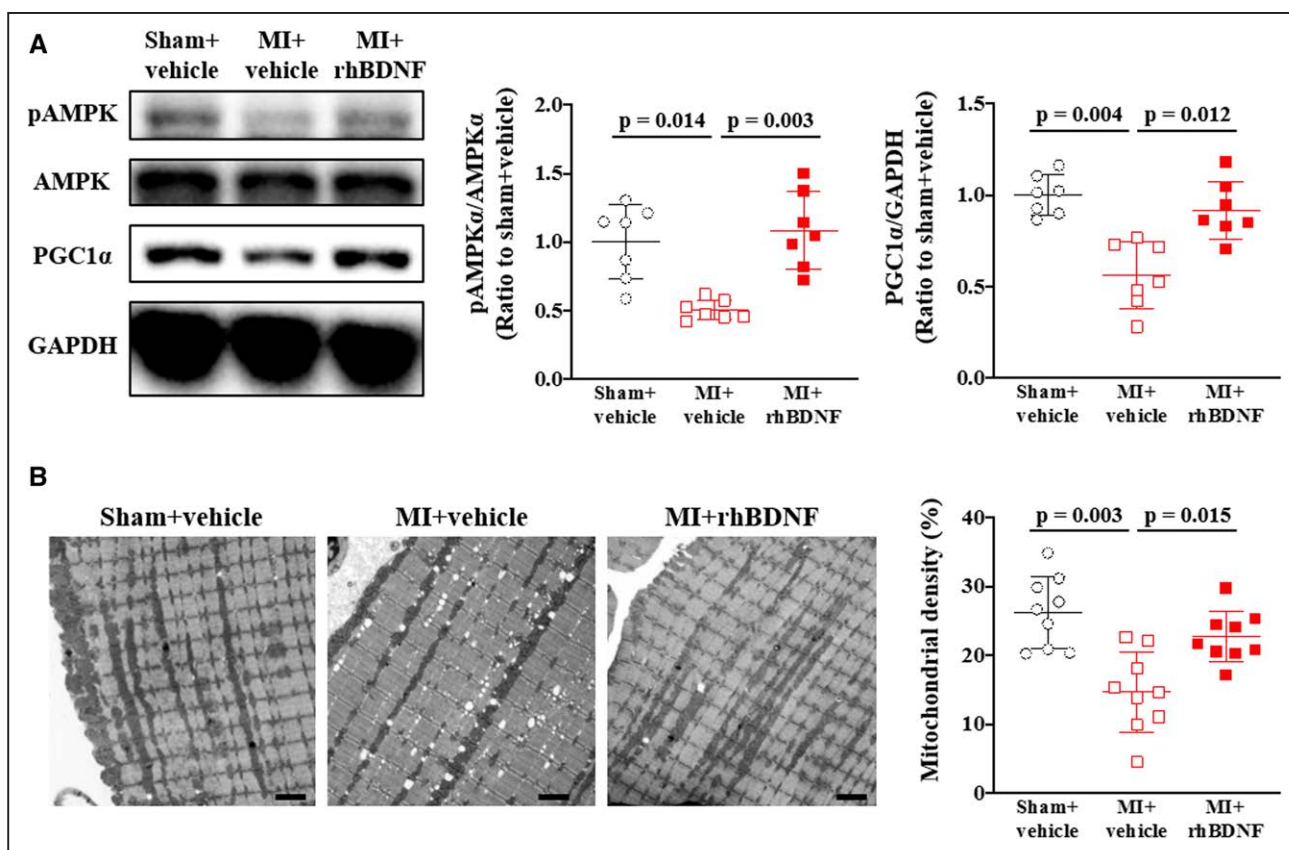


Figure 3. rhBDNF (recombinant human brain-derived neurotrophic factor) treatment improved AMPK α -PGC1 α signaling and mitochondrial biogenesis.

A, Representative Western blots and summary data of phosphorylated-AMPK α and PGC1 α in gastrocnemius muscle in the 3 experimental groups. $n=7$ per group. **B**, Representative transmission electron microscopy images in gastrocnemius muscle and summary data of mitochondria density. Nine images from 3 mice per group were analyzed. Scale bar, 2 μ m. $n=9$ per group. Data are mean \pm SD. MI indicates myocardial infarction.

and fatty acid oxidation; these changes are comparable to the effects of ET (Figure 6C).

The Effects of rhBDNF Were Inhibited by an AMPK α Inhibitor In Vitro

We confirmed the signal of BDNF with the use of C2C12 myotubes. The rhBDNF treatment of C2C12 myotubes increased the expressions of genes related to mitochondrial biogenesis and fatty acid oxidation, and these increases were completely inhibited by the addition of compound C, a selective inhibitor of AMPK α (Figure 6D), or anti-TrkB receptor antibody (Figure 6E).

DISCUSSION

The results of our experiments demonstrated that BDNF was abundant in oxidative fibers from mice. Taking our present findings into account together with the previous observation that BDNF expression was decreased in the skeletal muscle of mice with HF after MI,¹¹ we suggest that BDNF plays an important role in the development of

skeletal muscle abnormalities and the reduction of exercise capacity in HF. The results of our present investigation also clarified that the beneficial effects of rhBDNF on the exercise capacity of HF mice were due to the enhancement of fatty acid oxidation via the activation of AMPK α -PGC1 α signaling pathways. The mediation of rhBDNF, which was shown to have the therapeutic effect of increasing exercise capacity, occurred through this signaling in vivo. This finding is also supported by the results of our experiments using BDNF^{+/-} mice and AICAR. We thus speculate that BDNF is an exercise mimetic that can be applied in vivo and for humans.

To our knowledge, this is the first demonstration that BDNF was preferentially expressed in mitochondria-rich oxidative muscles rather than glycolytic muscles (Figure 1A through 1C). Skeletal muscle is a unique organ that has various fiber types, and it is important to know why BDNF is abundant in slow-twitch muscle fibers. Our immunofluorescence staining also showed that BDNF was co-localized with mitochondria (Figure 1D). We thus consider it possible that BDNF acts directly on mitochondria and can regulate the mitochondrial function in skeletal muscle.

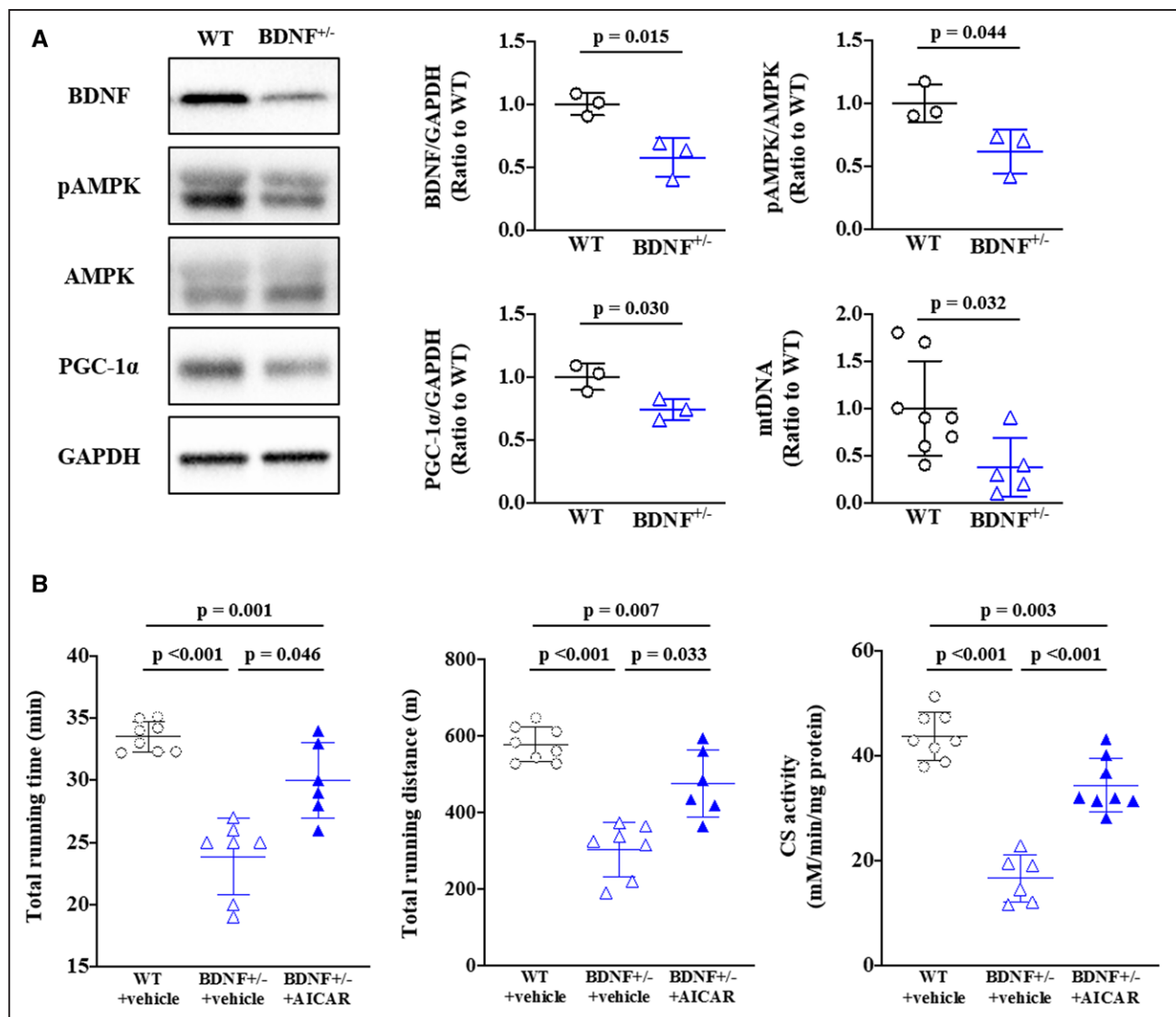


Figure 4. 5-aminoimidazole-4-carboxamide-1-beta-d-ribofuranoside (AICAR) improved the reduced exercise capacity and the mitochondrial function in skeletal muscle of the BDNF^{+/-} (brain-derived neurotrophic factor) mice.

A, Representative Western blots and summary data of BDNF, phosphorylated-AMPK α , PGC1 α , and mtDNA in gastrocnemius muscle in wild type (WT) and BDNF^{+/-} mice. n=3 per group for Western blots and n=8, and 5 for mtDNA. **B**, Total running time and total running distance to exhaustion. **C**, CS (citrate synthase) activity in skeletal muscle in WT+vehicle, BDNF^{+/-}+vehicle, and BDNF^{+/-}+AICAR mice. n=8, 7, and 6. Data are mean \pm SD. AICAR denotes activator of AMPK.

In the field of neurology, it is known that BDNF binding to TrkB receptors induces TrkB dimerization and autophosphorylation at specific tyrosine residues in the cytoplasmic domain, creating docking sites for adaptor proteins that trigger the activation of downstream signaling pathways.²¹ The increased expressions of genes related to mitochondrial biogenesis and fatty acid oxidation in C2C12 cells treated with BDNF were completely inhibited by the addition of anti-TrkB receptor antibody (Figure 6E). This result suggested that the effects of BDNF were dependent of TrkB receptors.

We also investigated whether rhBDNF phosphorylated TrkB receptors in the skeletal muscle. For this purpose, we performed Western blotting using 2 commercially

available antiphosphorylated receptor antibodies, and the results revealed no differences in the TrkB receptor phosphorylation level among the groups of sham+vehicle, MI+vehicle, and MI+rhBDNF mice (data not shown). We then used the Blue Native polyacrylamide gel electrophoresis method to further investigate whether BDNF and the TrkB receptors formed complexes in the skeletal muscle. The results showed that, indeed, BDNF and the TrkB receptors formed complexes, and these complexes were decreased in MI mice compared with sham mice (data not shown).

It was reported that clathrin-dependent endocytosis of TrkB-BDNF complexes is associated with Akt-mediated neuronal protection and dendritic growth.²²

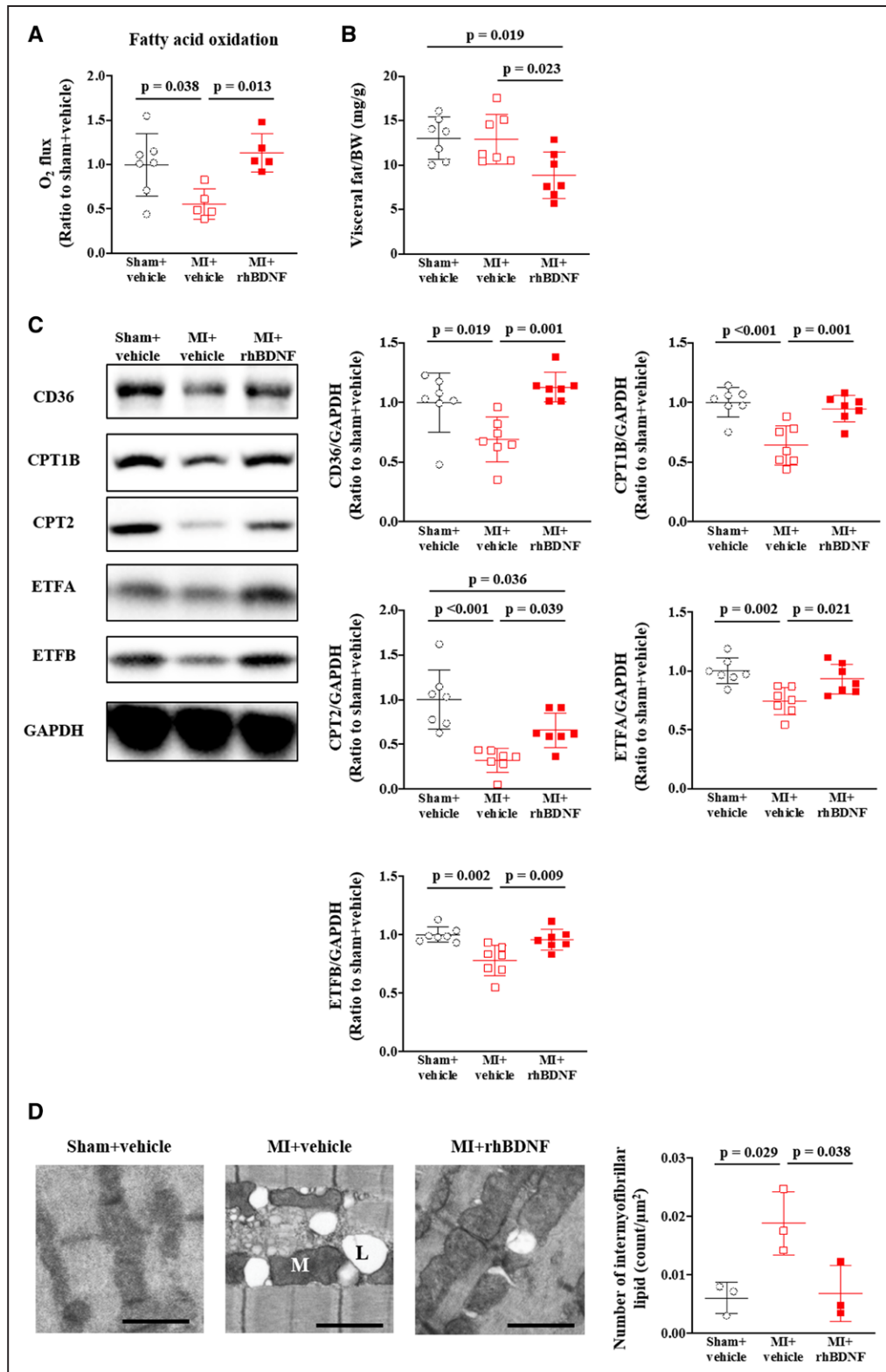


Figure 5. rhBDNF (recombinant human brain-derived neurotrophic factor) treatment enhanced the fatty acid oxidation in the skeletal muscle of myocardial infarction (MI) mice.

A, Mitochondrial oxygen consumption rates during state 3 (ADP-stimulated respiration) with fatty acids in permeabilized gastrocnemius muscle fibers. Values are relative to the O_2 flux of sham+vehicle mice. $n=7$, 5, and 5. **B**, Visceral fat (epididymal fat) weight/body weight (BW) in each group. $n=7$ per group. **C**, Representative Western blots and summary data of cluster of differentiation 36 (CD36), CPT (carnitine palmitoyl-transferase) 1B, CPT2, ETF A (electron transfer flavoprotein subunit α), and ETF B (electron transfer flavoprotein subunit β). Values were normalized by GAPDH. $n=7$ per group. **D**, Representative transmission electron microscopy images of skeletal muscle from MI+vehicle and MI+rhBDNF mice. Scale bar, 1 μm . Data are mean \pm SD.

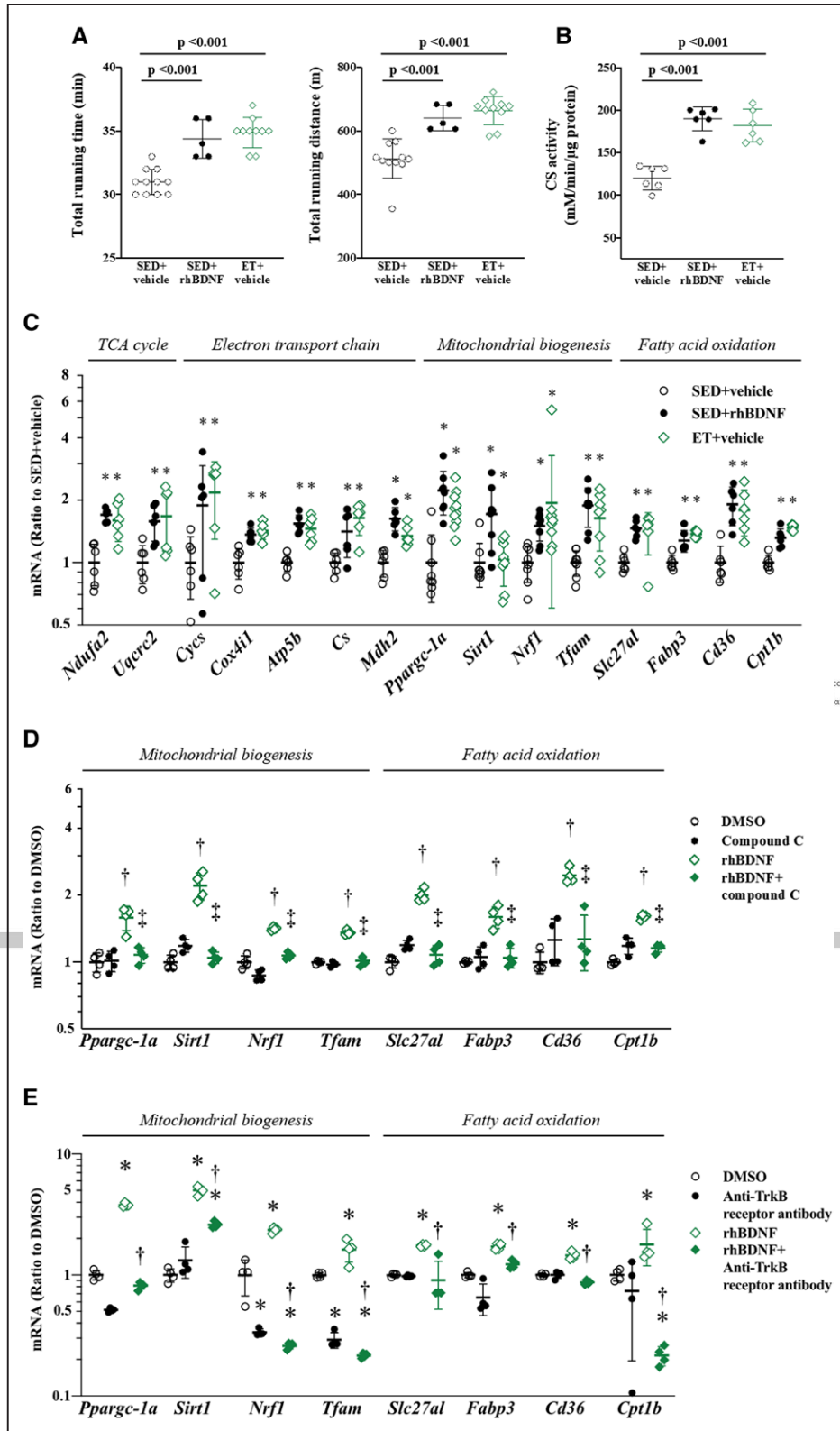


Figure 6. Beneficial effects of rhBDNF (recombinant human brain-derived neurotrophic factor) are equivalent to exercise training (ET).

A, Total running time and running distance to exhaustion (n=11, 5, and 10), **(B)** CS (citrate synthase) activity in the skeletal muscle (n=6 per group), and **(C)** gene expressions in the skeletal muscle from sedentary conditions (SED)+vehicle, SED+rhBDNF, and ET+vehicle mice (n=6, 7, and 8). **D**, Gene expressions in C2C12 myotubes treated with DMSO, compound C, rhBDNF, or rhBDNF+compound C (n=4 per group). **E**, Gene expressions in C2C12 myotubes treated with DMSO, anti-TrkB receptor antibody, rhBDNF, or rhBDNF+anti-TrkB receptor antibody (n=4 per group). Data are mean \pm SEM. *P<0.05 vs SED+vehicle. †P<0.05 vs DMSO. ‡P<0.05 vs rhBDNF.

The same mechanism may thus be associated with the downstream signaling of BDNF in the skeletal muscle. On the contrary, it is known that BDNF-activated TrkB mediates hippocampal plasticity via recruitment of phospholipase C and by subsequent phosphorylation of Ca²⁺-calmodulin-regulated protein kinase.²³ This may be associated with the increased phosphorylation of AMPK α by BDNF in the skeletal muscle. However, further experiments are necessary to clarify the details of these molecular mechanisms.

Our present findings also demonstrated that the treatment with rhBDNF increased the fatty acid oxidation in mouse gastrocnemius muscle (Figure 5A). It was reported that BDNF enhanced fatty acid oxidation in vitro (in intact L6 myotubes) and ex vivo (in isolated intact rat skeletal muscle).¹⁰ We expanded those findings in the present in vivo study, by demonstrating that rhBDNF could improve the impaired mitochondrial fatty acid oxidation in the skeletal muscle from mice with HF. This improvement was caused by an upregulation of fatty acid transport proteins and ETF rather than individual β -oxidation proteins (Figure 5).

In regard to the impaired fatty acid oxidation, we also observed accumulated lipid droplets in skeletal muscle by transmission electron microscopy (Figure 5D). Our prior research revealed that the level of intramyocellular lipid was increased in the skeletal muscle of patients with HF with lowered exercise capacity.⁴ Not only a low energy supply but also lipotoxicity in skeletal muscle may adversely affect exercise capacity in MI mice.²⁴ It is thus conceivable that BDNF may be beneficial for patients with other diseases with lipotoxicity in the skeletal muscle, such as type 2 diabetes.

In the present study, we used BDNF^{+/-} mice with an \approx 50% reduction in BDNF expression of the skeletal muscle, and this reduction was comparable to that of MI mice. The decreased exercise capacity of BDNF^{+/-} mice was improved by AICAR, a specific activator of AMPK, strongly supporting the possibility that AMPK α plays an important role in the downstream signaling of BDNF. AICAR is a cell-permeable precursor to ZMP, which mimics AMP, and it binds to the AMPK γ subunits and directly activates AMPK. Little is known about AICAR other than the AMPK-dependent effects of AICAR. Increased AMP due to the application of AICAR may reduce intracellular cAMP and suppress PKA-dependent signals. However, we could not clarify this issue in the present study.

The beneficial effects of the present rhBDNF treatment occurred via the same signaling pathway in the skeletal muscle as that affected by ET. Indeed, the 5-week rhBDNF treatment showed effects on exercise capacity and mitochondrial function that were equivalent to those achieved with 5 weeks of swimming training in mice (Figure 6). Some patients with HF cannot undergo sufficient ET because of their highly impaired skeletal muscle

abnormalities. Treatment with rhBDNF may become a pharmacological therapy that improves exercise capacity and prognosis in patients with HF, as an alternative or adjunct to ET. However, we cannot completely exclude the beneficial effects of rhBDNF on cardiac function. Although rhBDNF did not affect echocardiographic parameters at rest or the histological data of the mice, it may improve their exercise capacity due to an improvement in cardiac reserve during exercise. Unfortunately, we could not measure the echocardiographic parameters immediately after the exercise by the mice, due to some technical reasons including the poor quality of echocardiographic images associated with elevated heart rate, the instability of the mice after exercise, and difficulties with the echocardiography pretreatment. Moreover, even if rhBDNF did not improve cardiac remodeling and function at rest, it may improve fatty acid oxidation and mitochondrial content in the heart as observed in the skeletal muscle, and it may improve the subsequent cardiac reserve during exercise. Further experiments focusing on cardiac metabolism and the cardiac reserve during exercise are needed.

In summary, the beneficial effects of BDNF on the exercise capacity of mice with HF are mediated through an enhancement of fatty acid oxidation via the activation of AMPK α -PGC1 α in the skeletal muscle. BDNF may become a potential therapeutic option to improve exercise capacity as an alternative or adjunct to ET.

ARTICLE INFORMATION

Received January 11, 2019; accepted October 6, 2020.

Affiliations

Department of Cardiovascular Medicine (J.M., S. Takada, T.F., H.N., N.K., S.M., W.M., I.N., A.F., T.Y., S.K.), Department of Cancer Pathology (S. Tanaka), and Department of Molecular Biology (H.H., H.S.), Faculty of Medicine and Graduate School of Medicine, Hokkaido University, Sapporo, Japan.

Acknowledgments

We thank Mami Sato, Miwako Yamane, Noriko Ikeda, and Yuki Kimura for their technical assistance. We also thank Isao Yokota for his valuable advice about statistical analysis. Dr Matsumoto, S. Takada, and Dr Kinugawa conceived and designed the research. Dr Matsumoto and S. Takada performed the data analysis and interpretation. S. Tanaka performed the transmission electron microscopy analysis. Dr Handa performed the confocal microscopy analysis. Dr Matsumoto, S. Takada, Dr Furihata, Dr Nambu, Dr Kakutani, Dr Maekawa, and Dr Nakano performed the other experiments. Dr Matsumoto, S. Takada, Dr Fukushima, Dr Sabe, and Dr Kinugawa analyzed and interpreted the data. Drs Mizushima and Yokota performed statistical analysis. S. Takada, Dr Furihata, Dr Sabe, and Dr Kinugawa handled funding and supervision. Dr Matsumoto, S. Takada, and Dr Kinugawa drafted the article. Dr Furihata, Dr Nambu, Dr Kakutani, Dr Maekawa, Dr Mizushima, Dr Nakano, Dr Fukushima, Dr Yokota, S. Tanaka, Dr Handa, and Dr Sabe made critical revision of the article for important intellectual content. All authors read and approved the final article.

Sources of Funding

This study was supported in part by the Japan Society for the Promotion of Science grant-in-aid for scientific research No. JP26350879 (to Dr Kinugawa), No. JP17K15979 (Dr Furihata), and No. JP17H04758 (S. Takada).

Disclosures

None.

REFERENCES

- Kinugawa S, Takada S, Matsushima S, Okita K, Tsutsui H. Skeletal muscle abnormalities in heart failure. *Int Heart J*. 2015;56:475–484. doi: 10.1536/ihj.15-108
- Okita K, Kinugawa S, Tsutsui H. Exercise intolerance in chronic heart failure—skeletal muscle dysfunction and potential therapies. *Circ J*. 2013;77:293–300. doi: 10.1253/circj.12-1235
- Drexler H, Riede U, Münzel T, König H, Funke E, Just H. Alterations of skeletal muscle in chronic heart failure. *Circulation*. 1992;85:1751–1759. doi: 10.1161/01.cir.85.5.1751
- Hirabayashi K, Kinugawa S, Yokota T, Takada S, Fukushima A, Suga T, Takahashi M, Ono T, Morita N, Omokawa M, et al. Intramyocellular lipid is increased in the skeletal muscle of patients with dilated cardiomyopathy with lowered exercise capacity. *Int J Cardiol*. 2014;176:1110–1112. doi: 10.1016/j.ijcard.2014.07.113
- Bibel M, Barde YA. Neurotrophins: key regulators of cell fate and cell shape in the vertebrate nervous system. *Genes Dev*. 2000;14:2919–2937. doi: 10.1101/gad.841400
- Lu B, Figurov A. Role of neurotrophins in synapse development and plasticity. *Rev Neurosci*. 1997;8:1–12. doi: 10.1515/revneuro.1997.8.1.1
- Thoenen H. Neurotrophins and neuronal plasticity. *Science*. 1995;270:593–598. doi: 10.1126/science.270.5236.593
- Fukushima A, Kinugawa S, Homma T, Masaki Y, Furihata T, Yokota T, Matsushima S, Abe T, Suga T, Takada S, et al. Decreased serum brain-derived neurotrophic factor levels are correlated with exercise intolerance in patients with heart failure. *Int J Cardiol*. 2013;168:e142–e144. doi: 10.1016/j.ijcard.2013.08.073
- Fukushima A, Kinugawa S, Homma T, Masaki Y, Furihata T, Yokota T, Matsushima S, Takada S, Kadoguchi T, Oba K, et al. Serum brain-derived neurotrophic factor level predicts adverse clinical outcomes in patients with heart failure. *J Card Fail*. 2015;21:300–306. doi: 10.1016/j.cardfail.2015.01.003
- Matthews VB, Aström MB, Chan MH, Bruce CR, Krabbe KS, Prelovsek O, Akerström T, Yfanti C, Broholm C, Mortensen OH, et al. Brain-derived neurotrophic factor is produced by skeletal muscle cells in response to contraction and enhances fat oxidation via activation of AMP-activated protein kinase. *Diabetologia*. 2009;52:1409–1418. doi: 10.1007/s00125-009-1364-1
- Matsumoto J, Takada S, Kinugawa S, Furihata T, Nambu H, Kakutani N, Tsuda M, Fukushima A, Yokota T, Tanaka S, et al. Brain-derived neurotrophic factor improves limited exercise capacity in mice with heart failure. *Circulation*. 2018;138:2064–2066. doi: 10.1161/CIRCULATIONAHA.118.035212
- Narkar VA, Downes M, Yu RT, Emblar E, Wang YX, Banayo E, Mihaylova MM, Nelson MC, Zou Y, Juguilon H, et al. AMPK and PPAR δ agonists are exercise mimetics. *Cell*. 2008;134:405–415. doi: 10.1016/j.cell.2008.06.051
- Cheng A, Wan R, Yang JL, Kamimura N, Son TG, Ouyang X, Luo Y, Okun E, Mattson MP. Involvement of PGC-1 α in the formation and maintenance of neuronal dendritic spines. *Nat Commun*. 2012;3:1250. doi: 10.1038/ncomms2238
- Kawai S, Takagi Y, Kaneko S, Kurosawa T. Effect of three types of mixed anesthetic agents alternate to ketamine in mice. *Exp Anim*. 2011;60:481–487. doi: 10.1538/expanim.60.481
- Takada S, Masaki Y, Kinugawa S, Matsumoto J, Furihata T, Mizushima W, Kadoguchi T, Fukushima A, Homma T, Takahashi M, et al. Dipeptidyl peptidase-4 inhibitor improved exercise capacity and mitochondrial biogenesis in mice with heart failure via activation of glucagon-like peptide-1 receptor signalling. *Cardiovasc Res*. 2016;111:338–347. doi: 10.1093/cvr/cvw182
- Pachon RE, Scharf BA, Vatner DE, Vatner SF. Best anesthetics for assessing left ventricular systolic function by echocardiography in mice. *Am J Physiol Heart Circ Physiol*. 2015;308:H1525–H1529. doi: 10.1152/ajpheart.00890.2014
- Yokota T, Kinugawa S, Hirabayashi K, Matsushima S, Inoue N, Ohta Y, Hamaguchi S, Sobirin MA, Ono T, Suga T, et al. Oxidative stress in skeletal muscle impairs mitochondrial respiration and limits exercise capacity in type 2 diabetic mice. *Am J Physiol Heart Circ Physiol*. 2009;297:H1069–H1077. doi: 10.1152/ajpheart.00267.2009
- Takada S, Kinugawa S, Hirabayashi K, Suga T, Yokota T, Takahashi M, Fukushima A, Homma T, Ono T, Sobirin MA, et al. Angiotensin II receptor blocker improves the lowered exercise capacity and impaired mitochondrial function of the skeletal muscle in type 2 diabetic mice. *J Appl Physiol (1985)*. 2013;114:844–857.
- Suga T, Kinugawa S, Takada S, Kadoguchi T, Fukushima A, Homma T, Masaki Y, Furihata T, Takahashi M, Sobirin MA, et al. Combination of exercise training and diet restriction normalizes limited exercise capacity and impaired skeletal muscle function in diet-induced diabetic mice. *Endocrinology*. 2014;155:68–80. doi: 10.1210/en.2013-1382
- Fukushima A, Kinugawa S, Takada S, Matsushima S, Sobirin MA, Ono T, Takahashi M, Suga T, Homma T, Masaki Y, et al. (Pro)renin receptor in skeletal muscle is involved in the development of insulin resistance associated with postinfarct heart failure in mice. *Am J Physiol Endocrinol Metab*. 2014;307:E503–E514. doi: 10.1152/ajpendo.00449.2013
- Huang EJ, Reichardt LF. Trk receptors: roles in neuronal signal transduction. *Annu Rev Biochem*. 2003;72:609–642. doi: 10.1146/annurev.biochem.72.12.609
- Zheng J, Shen WH, Lu TJ, Zhou Y, Chen Q, Wang Z, Xiang T, Zhu YC, Zhang C, Duan S, et al. Clathrin-dependent endocytosis is required for TrkB-dependent Akt-mediated neuronal protection and dendritic growth. *J Biol Chem*. 2008;283:13280–13288. doi: 10.1074/jbc.M709930200
- Minichiello L, Calella AM, Medina DL, Bonhoeffer T, Klein R, Korte M. Mechanism of TrkB-mediated hippocampal long-term potentiation. *Neuron*. 2002;36:121–137. doi: 10.1016/s0896-6273(02)00942-x
- Morales PE, Bucarey JL, Espinosa A. Muscle lipid metabolism: role of lipid droplets and perilipins. *J Diabetes Res*. 2017;2017:1789395. doi: 10.1155/2017/1789395

1 *Data Supplement*

2 **Brain-derived neurotrophic factor improves lowered mitochondrial biogenesis and**
3 **fatty acid oxidation via the activation of AMPK α -PGC1 α signaling in skeletal muscle of**
4 **mice with heart failure**

5 **Short title:** BDNF and AMPK α -PGC1 α signaling in skeletal muscle

6

7 **Authors:** Junichi Matsumoto^{1†}, MD, PhD; Shingo Takada^{1†}, PhD; Takaaki Furihata¹, MD,
8 PhD; Hideo Nambu¹, MD, PhD; Naoya Kakutani¹, PhD; Satoshi Maekawa¹, MD, PhD;
9 Wataru Mizushima¹, MD, PhD; Ippei Nakano¹, MD, PhD; Arata Fukushima¹, MD, PhD;
10 Takashi Yokota¹, MD, PhD; Shinya Tanaka², MD, PhD; Haruka Handa³, MD, PhD;
11 Hisataka Sabe³, PhD; and Shintaro Kinugawa^{1*}, MD, PhD

12

1 **Supplemental Methods**

2 *Western blotting and antibodies*

3 Skeletal muscle samples were homogenized in ice-cold Cell lysis buffer (Cell Signaling
4 Technology [CST], Beverly, MA) supplemented with Complete protease inhibitor cocktail
5 (Roche, Mannheim, Germany), 1 mM phenylmethylsulfonyl fluoride, and PhosSTOP
6 phosphatase inhibitor cocktail (Roche). After homogenization using a Polytron homogenizer
7 and centrifugation at 15,000 g for 20 min at 4°C, we collected the supernatant. Samples were
8 diluted with 2× sample buffer in addition to 2-mercaptoethanol and then heated at 100°C for
9 3 min.

10 Samples (20–40 µg of total protein) were applied on a Criterion TGX Precast Gel
11 (Bio-Rad Laboratories, Hercules, CA) and electrophoretically separated by sodium dodecyl
12 sulfate-polyacrylamide gel electrophoresis. Gels were transferred onto a poly vinylidene di-
13 fluoride membrane using the Trans-Blot Turbo Transfer System (Bio-Rad Laboratories). The
14 membranes were blocked at room temperature for 1 hr in 5% non-fat dry milk in TBS-T
15 buffer (Tris-buffered saline containing 0.1% Tween 20). They were incubated using primary
16 antibodies against BDNF (1:1,000, ab108319, Abcam, Cambridge, MA), p-AMPK α
17 (Thr172) (1:1,000, #2535, CST), AMPK α (1:2000, #2532, CST), PGC1 α (1:500, ab77210,
18 Abcam), GAPDH (1:5,000, #3683, CST), CD36 (1:1,000, ab133625, Abcam), CPT1B
19 (1:1,000, ab134988, Abcam), CPT2 (1:1,000, ab71435, Abcam), ETFA (1:1,000, ab110316,
20 Abcam), and ETFB (1:1,000, ab104944, Abcam) in 5% milk/TBS-T overnight at 4°C.

21 After being washed with TBS-T at least three times, the membranes were incubated
22 with a horseradish peroxidase-conjugated secondary antibody at room temperature for 1 hr at a
23 dilution of 1:5,000 in 5% milk/TBS-T. After washing, the membranes were developed with
24 ECL or ECL Prime Western Blotting Detection Reagent (GE Healthcare, Little Chalfont,
25 UK) or SuperSignal West Femto (Thermo Fisher Scientific, Waltham, MA) and then

1 processed for detection with a ChemiDoc XRS+ System (Bio-Rad Laboratories). We used
2 GAPDH as a loading control. The density of the signals of bands was quantified with Image
3 J software (U.S. National Institutes of Health).

4

5 *Immunohistochemical staining*

6 Skeletal muscle samples were immediately embedded in OCT compound (Thermo Fisher
7 Scientific), then frozen in melting isopentane precooled in liquid nitrogen. The frozen
8 sections of gastrocnemius and soleus muscles were cut into 12- μ m-thick sections with a
9 cryostat (HM500-OM, Microm, Walldorf, Germany). The method of succinate
10 dehydrogenase (SDH) staining was as described.¹ For BDNF staining, slides were fixed with
11 ice-cold 4% paraformaldehyde for 7 min, washed with PBS and fixed with 0.3% H₂O₂ in
12 methanol for 30 min. After being washed again with PBS, the slides were incubated with
13 anti-BDNF primary antibody diluted at 1:300 overnight at 4°C. After being washed with
14 PBS, the slides were incubated with EnVision+ HRP Labelled Polymer Anti-Rabbit (K4002;
15 Dako, Carpinteria, CA) for 30 min. Staining was visualized by incubation for 7 min in a
16 Dako Liquid DAB substrate-chromagen system (K3466; Dako). The sections were then
17 imaged using a BZ-X700 microscope (Keyence, Tokyo).

18

19 *Immunofluorescence microscopy*

20 The immunofluorescence microscopy analysis was performed as described.² Briefly, C2C12
21 myotubes were plated onto cover-glasses coated with 50 μ g/ml fibronectin. After 24-hr
22 incubation at 37°C, the cells were fixed with 2% formaldehyde in PBS at 37°C for 10 min,
23 followed by ice-cold methanol for a 5-min fixation at -20°C. After blocking with 1% bovine
24 serum albumin (BSA) in PBS for 30 min, the samples were incubated with antibodies
25 against BDNF (1:800, ab108319, Abcam) and MTCO1 (1:200, ab14705, Abcam) in 1%

1 BSA/PBS overnight at 4°C. After being rinsed with blocking buffer, the samples were
2 incubated with secondary antibodies conjugated with Alexa 488 (against rabbit IgG) and
3 Alexa 555 (against mouse IgG) fluorescent dyes at a dilution of 1:1,000 for 30 min at room
4 temperature.

5 Nuclei were stained with TO-PRO-3 (Thermo Fisher Scientific) at a dilution of 1:1,000.

6 Fluorescence images were obtained with a confocal laser-scanning microscope using a 100×

7 H oil-immersion objective (NA of 1.4; CFI Plan Apo VC; Nikon, Tokyo) and analyzed with

8 the attached software (model A1R with NIS-Elements). We performed a high-resolution

9 structured illumination microscopy (SIM) analysis to examine the co-localization of BDNF

10 and mitochondria using the N-SIM microscope (Nikon) and NIS-Elements software (Nikon).

11

12 *Citrate synthase activity*

13 The enzymatic activity of citrate synthase (CS, a key enzyme of the tricarboxylic acid
14 [TCA] cycle) was spectrophotometrically determined in the tissue homogenate from skeletal
15 muscle samples as described.³

16

17 *Transmission electron microscopy*

18 Each muscle sample was fixed in 3% glutaraldehyde with 0.1 mM phosphate buffer and

19 postfixed in 0.1 mM phosphate buffer with 1% osmium tetroxide and then serially

20 dehydrated in ethanol and embedded in epoxy resin. Sections were cut on an ultramicrotome

21 (LKB, Brommer, Sweden), and consecutive ultrathin sections were mounted on copper

22 grids. The ultrathin sections were stained and examined with an electron microscope (H-

23 7100; Hitachi, Tokyo).³

24

25 *Mitochondrial DNA analysis*

1 To determine mitochondrial DNA content, DNA was isolated from frozen muscle samples
2 using the DNAeasy tissue kit (Qiagen, Valencia CA USA). DNA was quantified
3 spectrophotometrically at 260 nm wavelength. The DNA was used to amplify cytochrome *b*
4 and GAPDH using quantitative real-time polymerase chain reaction (PCR). The cytochrome
5 *b* primer probe was generated by using the following sequence: forward primer
6 TATTCCTTCATGTCGGACGA, reverse primer AAATGCTGTGGCTATGACTG, and
7 probe ACCTGAAACATTGGAGTACTTCTACTG.

8

9 *Real-time PCR analysis*

10 Total RNA was extracted from frozen muscle samples or cultured C2C12 myotubes with
11 QuickGene-810 (FujiFilm, Tokyo) according to the manufacturer's instructions.³ The
12 extracted RNA was quantified spectrophotometrically at 260 nm. cDNA was synthesized
13 with a High-Capacity cDNA Reverse Transcription Kit (Applied Biosystems, Foster City,
14 CA). Reverse transcription was performed at 25°C for 10 min, 37°C for 120 min, and 85°C
15 for 5 sec, and then cooled at 4°C. cDNA samples were stored at -20°C until subsequent
16 amplification.

17 A TaqMan quantitative real-time polymerase chain reaction (PCR) was performed
18 with the 7300 real-time PCR system (Applied Biosystems) with TaqMan Gene Expression
19 Master Mix (Applied Biosystems). The TaqMan primers and probes used are listed in
20 **Supplemental Table S2**. Following 2 min at 50°C and 10 min at 95°C, the PCR
21 amplification was performed for 40 cycles, with each cycle at 95°C for a 15-sec denaturing
22 step and 60°C for 1 min annealing/extending step. GAPDH was used as an internal control.
23 mRNA expression was normalized by the GAPDH expression levels in each sample.^{15,21}

24

1 **Supplemental Table S1. Organ weight and echocardiography in sham+vehicle,**
2 **MI+vehicle, and MI+rhBDNF mice.**

	Sham+vehicle	MI+vehicle	MI+rhBDNF
n	7	7	7
BW (g)	25.6 ± 0.8	26.3 ± 1.0	24.2 ± 0.8*†
Food intake (g/day)	2.8 ± 0.8	3.2 ± 0.5	2.9 ± 0.3
Organ weights			
Heart weight/BW (mg/g)	4.6 ± 0.5	6.4 ± 1.3*	6.6 ± 0.8*
LV weight/BW (mg/g)	3.2 ± 0.5	3.9 ± 0.3*	4.4 ± 0.3*
Lung weight/BW (mg/g)	5.3 ± 0.5	8.1 ± 3.7	8.1 ± 1.8
Gastrocnemius weight/BW (mg/g)	5.5 ± 0.3	5.4 ± 0.3	5.4 ± 0.3
Soleus weight/BW (mg/g)	0.41 ± 0.03	0.40 ± 0.03	0.42 ± 0.03
Echocardiography			
Heart Rate (bpm)	703 ± 13	681 ± 29	684 ± 26
LV end-diastolic diameter (mm)	3.2 ± 0.3	5.4 ± 0.3*	5.2 ± 0.5*
LV end-systolic diameter (mm)	1.7 ± 0.3	4.9 ± 0.3*	4.7 ± 0.8*
% fractional shortening (%)	47.4 ± 5.0	8.7 ± 2.1*	9.8 ± 2.9*
LV anterior wall thickness (mm)	0.70 ± 0.03	0.31 ± 0.08*	0.29 ± 0.08*
LV posterior wall thickness (mm)	0.73 ± 0.05	1.10 ± 0.08*	1.04 ± 0.13*

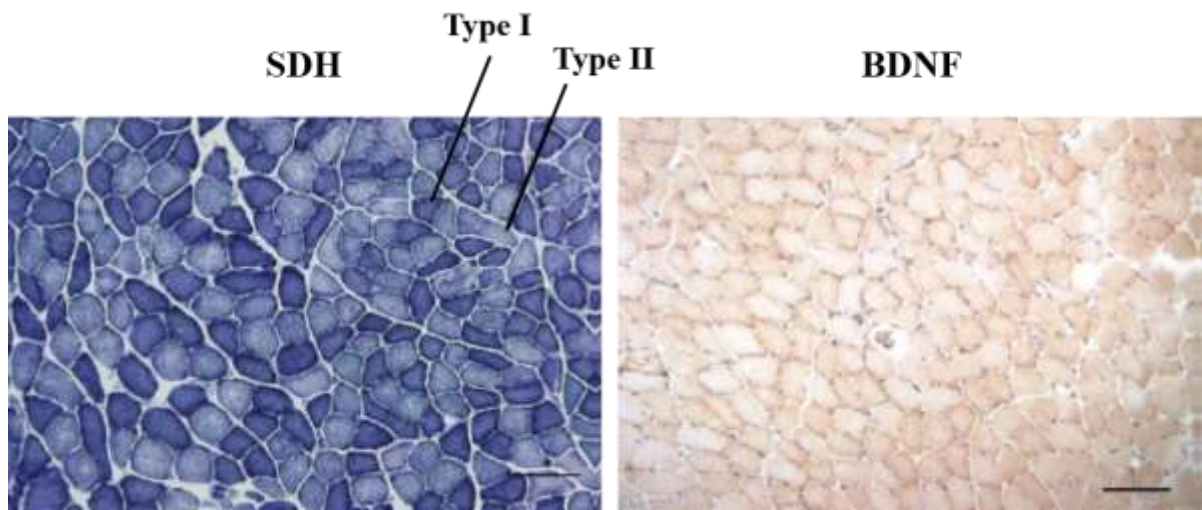
1 Data are mean±SD. * $P < 0.05$ vs. sham+vehicle, † $P < 0.05$ vs. MI+vehicle. bpm: beats per
2 minute, BW: body weight, V: left ventricle.
3

1 **Supplemental Table S2. TaqMan gene expression assays**

Gene	Assay-ID	Reference sequence	Exon boundary	Amplicon length
<i>Atp5b</i>	Mm00443967_g1	NM_016774.3	4-5	83
<i>Cox4i1</i>	Mm01250094_ml	NM_009941.2	2-3	116
<i>Cpt1b</i>	Mm00487191_ml	NM_009948.2	8-9	88
<i>Cs</i>	Mm00466043_ml	NM_026444.3	1-2	57
<i>Cycs</i>	Mm01621048_s1	NM_007808.4	3-3	119
<i>Fabp3</i>	Mm02342495_ml	NM_010174.1	3-4	94
<i>Fatp1</i>	Mm00449511_ml	NM_011977.3	8-9	66
<i>Mdh2</i>	Mm00725890_s1	NM_008617.2	4-4	71
<i>Ndufa2</i>	Mm00477755_g1	NM_010885.4	1-2	81
<i>Ppargc1α</i>	Mm01208835_ml	NM_008904.2	7-8	68
<i>Sirt1</i>	Mm01168521_ml	NM_019812.2	2-3	96
<i>Tfam</i>	Mm00447485_ml	NM_009360.4	2-3	81
<i>Uqcrc2</i>	Mm00445961_ml	NM_025899.2	6-7	84
<i>Gapdh</i>	Mm03302249_g1	NM_008084.2	1-1	70

2

1 **Supplemental Fig. S1. BDNF expressions in the soleus muscle**



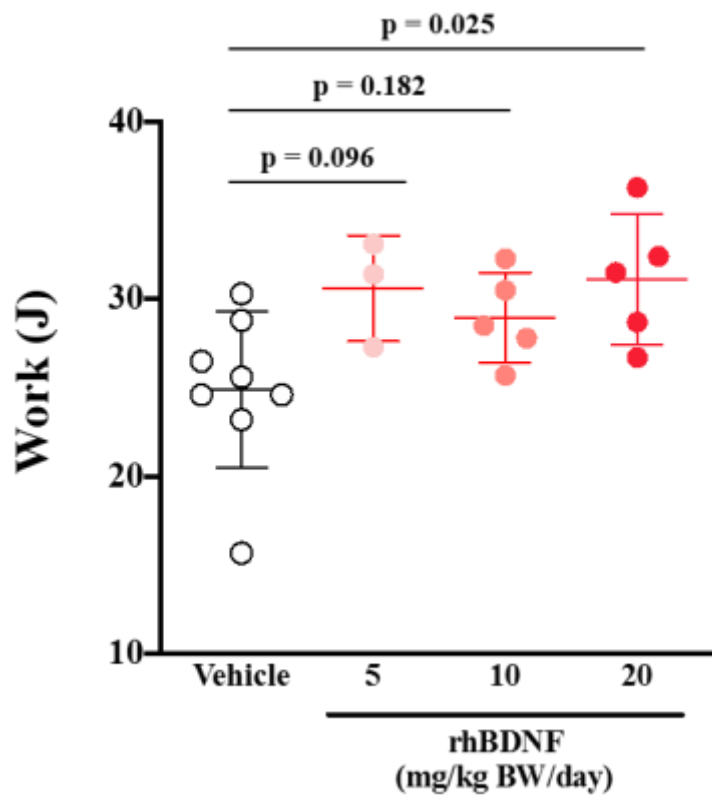
2

3 Representative immunohistochemical staining images for SDH (left panel) and BDNF (right

4 panel) in the soleus muscle. Scale bar, 100 μ m.

5

1 Supplemental Fig. S2. Effect of various dose of rhBDNF on Work



2

3 Exercise capacity (Work to exhaustion) in C57B6/6J mice treated with vehicle or various

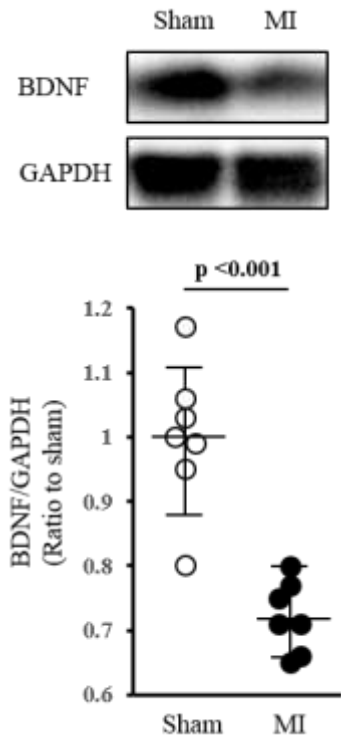
4 dose of rhBDNF (5, 10, and 20 mg/kg body weight/ day). n=8, 3, 5, and 5. Data are

5 mean±SD. BW; body weight.

6

7

1 **Supplemental Fig. S3. BDNF expression in the skeletal muscle was decreased in MI**
2 **mice.**



3

4 Representative Western blots and summary data of BDNF in gastrocnemius muscle in Sham
5 and MI mice. n=7 per group. Data are mean±SD.

6

1 **Supplemental References**

- 2 1. Suga T, Kinugawa S, Takada S, Kadoguchi T, Fukushima A, Homma T, Masaki Y,
3 Furihata T, Takahashi M, Sobirin MA, Ono T, Hirabayashi K, Yokota T, Tanaka S,
4 Okita K, Tsutsui H. Combination of exercise training and diet restriction normalizes
5 limited exercise capacity and impaired skeletal muscle function in diet-induced diabetic
6 mice. *Endocrinology*. 2014;155:68–80.
- 7 2. Onodera Y, Nam JM, Horikawa M, Shirato H, Sabe H. Arf6-driven cell invasion is
8 intrinsically linked to TRAK1-mediated mitochondrial anterograde trafficking to avoid
9 oxidative catastrophe. *Nat Commun*. 2018;9:2682.
- 10 3. Takada S, Masaki Y, Kinugawa S, Matsumoto J, Furihata T, Mizushima W, Kadoguchi
11 T, Fukushima A, Homma T, Takahashi M, Harashima S, Matsushima S, Yokota T,
12 Tanaka S, Okita K, Tsutsui H. Dipeptidyl peptidase-4 inhibitor improved exercise
13 capacity and mitochondrial biogenesis in mice with heart failure via activation of
14 glucagon-like peptide-1 receptor signalling. *Cardiovasc Res*. 2016;111:338–347.
- 15